

Three-Phase Modeling of Dynamic Kill in Gas-Condensate Well Using Advection Upstream Splitting Method Hybrid Scheme

Abouzar Daneshpajouh and Saeed Shad*

Chemical and Petroleum Engineering Department, Sharif University of Technology, Tehran, Iran

ABSTRACT

Understanding and modeling of three-phase transient flow in gas-condensate wells play a vital role in designing and optimizing dynamic kill procedure of each well that needs to capture the discontinuities in density, geometry, and velocity of phases but also the effect of temperature on such parameters. In this study, two-phase Advection-Upstream-Splitting-Method (AUSMV) hybrid scheme is extended to a three-phase model capable of modeling blowout and dynamic kill in gas-condensate-water wells. In order to better understand and model such a process, density and viscosity changes are calculated using the Peng-Robinson equation of state. Moreover, the resulted simulator enables us to study and model highly changing flow conditions during blowout and dynamic kill process applied to a well in a gas condensate reservoir. In addition, a sensitivity analysis has been conducted on the relief well kill rate, pump step down schedule, and well intersection depth. Moreover, the results reveal the impact and influence of each of these parameters on dynamic kill process. Finally, the model introduced here and the results of the sensitivity analysis using this transient three-phase model can be used to better design a control process for wells in gas condensate reservoirs.

Keywords: Three Phase Modeling, Dynamic Kill, Gas-Condensate Well, Advection Upstream Splitting Method, Hybrid Scheme.

INTRODUCTION

The dynamic kill is a procedure to regain control of a surface or underground blowout. It involves pumping kill fluid through either a relief well or an injection string into a blowing well. Moreover, the used pump rate must create enough back pressure to exceed the shut in formation pressure and stop the uncontrolled flow of fluids and hydrocarbons from the wells. The provided back

pressure depends on frictional pressure losses and hydrostatic pressure due to the multiphase flow of formation and kill fluids through the wellbore.

Transient multiphase flow simulators are widely used for designing contingency plans and relief well designs. The ability to accurately predict the behavior of blowing well and designing control responses have a significant impact on saving assets and environment. Mathematical models used in

*Corresponding author

Saeed Shad

Email: saeed.shad@sharif.edu

Tel: +98 21 6616 6456

Fax: +98 21 4269 3517

Article history

Received: March 18, 2018

Received in revised form: August 26, 2018

Accepted: November 26, 2018

Available online: May 21, 2019

DOI: 10.22078/jpst.2018.3230.1515

such simulators consist of two major components: flow through reservoirs to the wellbore and fluid flow inside the wellbore itself. In order to achieve a better and more realistic understanding of dynamic kill, the wellbore and reservoir models should be coupled. This is due to the fact that any variation in the flow conditions in the wellbore will inevitably cause a change in inflow from the reservoir and vice versa.

In the past, calculation of kill parameters of blowing well has received significant attention. A landmark model for an on-bottom dynamic kill of a surface blowout was first presented by Blount and Soeimah in 1978 based on the steady state flow assumption. It was successfully used during kill operations on Arun field blowout in Indonesia. In their work, a formula was developed by them for Initial kill fluid density, kill fluid injection rate, size of the relief well, and the required hydraulic horsepower of the pump. Moreover, the steady state system analysis approach was developed by Lynch et al for a dynamic kill to bring under control a CO₂ near bottom blowout that occurred in 1982. Moreover, a systematic technique for handling shallow gas flows based on an on the bottom dynamic kill was developed by Koederitz et al in 1987. In addition, the planning of kill operation using of the dynamic two-phase pipe flow simulator OLGAs was described by Rygg et al in 1990. Also, three methods for determining the upper and lower limits of the injection rate needed to dynamically kill a well were presented by Kouba et al in 1993. These include a technique for establishing a conservative which is the most probable minimum kill rate. In addition, a dynamic kill computer program based on steady state system analysis for controlling surface blowouts was developed by Al-Shheri in 1994.

The model simulates multiphase flow with the aid of the Beggs and Brill correlation in blowout and relief wells, and predicts and links the expected reservoir performance with wellbore hydraulics. Moreover, a methodology for predicting blowout rates from sour-gas wells was presented by Kikani et al in 1996. The blowout rates have been calculated by superimposing reservoir and tubing performance curves based on steady-state correlations.

In addition, a full-scale field test to study a dynamic kill in a high rate gas well was designed, executed, and analyzed by Oudeman in 1998. Several tests were carried out at different flow conditions. After analyzing the test results, the authors proposed equations to predict the following kill parameters for a successful and efficient kill job.

Also, a set of equations for determining the pump rate has been developed by Wessel and Tarr in 1991 to stop the flow with either an infinite volume of kill mud or when the first kill mud reaches the fractured formation. The derivations or references assumed homogeneous multi-phase flow. In addition, a computational method using a two-phase wellbore simulator that handles mass, momentum, and energy transports, leading to the estimation of blowout rate in a given wellbore-reservoir system was developed by Hassan et al in 2000. An ultra-deep well control using the dynamic kill technique was studied by Noynaert et al in 2005. In addition, their study was conducted using a newly developed dynamic kill simulator, COMASim, to model blowout initial conditions and blowout control in simple wellbore geometries. Most of the mentioned works used steady state models to predict flow parameters or transient models based on the finite difference method.

Since blowout in the gas-condensate well is highly transient phenomena, the need for a robust fast numerical method capable of capturing discontinuity in fluid density and pressure is crucial. Thus in this study, focus is on Hybrid flux-splitting schemes for solving the compressible Euler and Navier-Stokes equations and advection upstream splitting method (AUSM) presented by Wada and Liou in 1994 [1]. This method was originally developed for the aviation industry and on this basis, a hybrid scheme termed the "advection upstream splitting model (AUSMV)" was proposed by Evje and Fjelde in 2003 [6]. Moreover, the "advection upstream splitting model (AUSMV)" solved a hyperbolic system of conservation laws for a one dimensional, two-phase model, in which the flow component perpendicular to a pipe or tube axis was averaged. Also, the capability of this model was demonstrated by Udegbumam et al in 2015 [2]; moreover, the model was used to handle highly changing flow scenarios with examples taken from managed pressure drilling and underbalanced operations. The model used in this study is an extension to the model which has been provided by Udegbumam et al in 2015, which computational efficiency of the method is presented in their article [2]. One of the assumptions made in this new proposed model is that the volume fraction of gas, condensate, and water remains constant in current simulation block, but by passing to next block, thermodynamic model predicts new volume fractions according to block temperature and calculated pressure; moreover, by using these methods, the effect of phase transformation is implemented.

The finite volume method is used to solve the governing equations. In addition, the advection

upstream splitting method (AUSM) type scheme is extended to three phase model to handle the nature of three phase flow in gas condensate well. Also, AUSMV (Advection Upstream Splitting Method) scheme and its hybrids have provided the oil and gas industry with a robust model that can handle dynamic flow systems required to investigate different drilling related flow and pressure control scenarios that can be used to better design the well control and managed pressure drilling procedures. The current study extends AUSMV scheme to the three-phase model enabling transient three phase simulation of gas condensate flow in blowing well. Moreover, gas-condensate reservoir is represented with a productivity index (PI) model and coupled with the flow model inside the wellbore.

The following equations represent the flow of gas and liquid from the reservoir into the well:

$$q = J_g (P_{\text{reservoir}}^2 - P_{\text{flowing well}}^2)^{0.5}$$

$$q = J_c (P_{\text{reservoir}} - P_{\text{flowing well}})$$

where J is the productivity index and q is the rate of fluid entering the wellbore. Two separate PI model acts at the same time.

Transient three-phase wellbore model based on conservation of mass, momentum, and energy is developed to model flow inside the wellbore based on finite volume method to solve governing equations using advection upstream splitting method (AUSM) type scheme.

In order to model temperature changes, the energy equation is solved with a time lag to flow model and temperature impact on flow model, density and viscosity are calculated using Peng Robinson equation of state. Updated fluid properties resulted from the equation of state calculation are used to update the flow model.

The capability of the model to predict the flow

parameters and transient behavior of dynamic kill process for optimizing kill design scenarios is demonstrated with a simulation case and sensitivity analysis in a gas condensate reservoir scenario.

EXPERIMENTAL PROCEDURE

Three-Phase Model

The three phase-model considered in this study is one dimensional, and it is based on drift flux formulation. In order to avoid calculating momentum exchange rate between phases, three mass conservation equations and a mixture momentum equation are coupled with each other. However, slip relation similar to those proposed by Soprano et al in 2010 is used to calculate the velocity of each phase [3]. The system of hyperbolic laws for the fluid-mass (gas, condensate, and water) and a mixture-momentum conservation is shown in equations 3a, 3b, 3c, and 4 respectively:

$$\frac{\partial(\alpha_g \rho_g)}{\partial t} + \frac{\partial(\alpha_g \rho_g v_g)}{\partial x} = \Gamma_g \tag{3a}$$

$$\frac{\partial(\alpha_c \rho_c)}{\partial t} + \frac{\partial(\alpha_c \rho_c v_c)}{\partial x} = \Gamma_c \tag{3b}$$

$$\frac{\partial(\alpha_w \rho_w)}{\partial t} + \frac{\partial(\alpha_w \rho_w v_w)}{\partial x} = \Gamma_w \tag{3c}$$

$$\frac{\partial(\alpha_g \rho_g v_g + \alpha_c \rho_c v_c + \alpha_w \rho_w v_w)}{\partial t} + \frac{\partial(\alpha_g \rho_g v_g^2 + \alpha_c \rho_c v_c^2 + \alpha_w \rho_w v_w^2 + P)}{\partial x} = -q \tag{4}$$

under the assumption of no mass exchange between the phases ($\Gamma_g = \Gamma_w = \Gamma_c = 0$), the equation system (3a-4) can be written in the following conservative vector form:

$$\frac{\partial w}{\partial t} + \frac{\partial F(w)}{\partial x} = S(w) \tag{5}$$

In which w , $F(w)$ and $S(w)$ are vectors as shown below:

$$w = \begin{pmatrix} w_g \\ w_c \\ w_w \\ w_m \end{pmatrix} = \begin{pmatrix} \rho_g \alpha_g \\ \rho_c \alpha_c \\ \rho_w \alpha_w \\ \alpha_g \rho_g v_g + \alpha_c \rho_c v_c + \alpha_w \rho_w v_w \end{pmatrix} \tag{6}$$

$$F(w) = \begin{pmatrix} v_g w_g \\ v_c w_c \\ v_w w_w \\ v_g^2 w_g + v_c^2 w_c + v_w^2 w_w + P \end{pmatrix} \tag{7}$$

$$S = \begin{pmatrix} 0 \\ 0 \\ 0 \\ -q \end{pmatrix} \tag{8}$$

Pressure and volume fractions are physical variables that depend on the conservative variables w_g , w_c and w_w . It is assumed that density is a function of pressure ($\rho = \rho(P)$), the unknown parameters for a system of gas, condensate, and water will consist of the following items: α_g , α_c , α_w , v_g , v_c , v_w and P . By the fact that there are seven different equations resulted from governing equations, the problem is well posed. In order to improve the simulation performance and to reduce the number of equations, the concept of drift-flux model (Hibiki and Ishii, 2003) has been adopted to the modeling; moreover, the concept of the drift-flux model has been presented by Hibiki and Ishii in 2003 [4]. Such a model uses the sum of momentum equations for all phases and introduces a mixture velocity, defined as

$$v_m = \frac{\alpha_g \rho_g v_g + \alpha_c \rho_c v_c + \alpha_w \rho_w v_w}{\rho_m} \tag{9}$$

And ρ_m is the mixture density given as:

$$\rho_m = \alpha_g \rho_g + \alpha_c \rho_c + \alpha_w \rho_w \tag{10}$$

Since the drift-flux model is a two-phase model, it is necessary to somehow extend this procedure for a three-phase system. The procedure is the same as described by Soprano et al in 2010 [3], i.e., splitting the three-phase system in two sub-systems: a gas-liquid and a condensate-water system, where the liquid phase is the sum of condensate and water phases [3].

Now, it is possible to assume that the velocity of

each phase in the gas-liquid system is a function of mixture velocity (v_m) and drift velocity between phases (v_d^{ij}). The following equations show the gas and liquid velocities accordingly:

$$v_g = v_m + \frac{\rho_l}{\rho_m} v_d^{gl} \quad (11)$$

$$v_l = v_m + \frac{\rho_g}{\rho_m} v_d^{gl} \quad (12)$$

The liquid phase itself consists of water and condensate. Therefore, following a similar approach, for the condensate-water system, phase velocities are given as:

$$v_c = v_l + \frac{\rho_w}{\rho_l} v_d^{cw} \quad (13)$$

$$v_w = v_l - \frac{\alpha_c \rho_c}{\alpha_l \rho_l} v_d^{cw} \quad (14)$$

Similar to that of mixture velocity and density, for the liquid phase we have:

$$v_l = \frac{\alpha_c \rho_c v_c + \alpha_w \rho_w v_w}{\rho_l} \quad (15)$$

$$\rho_l = \alpha_c \rho_c + \alpha_w \rho_w \quad (16)$$

The drift velocity for a liquid-gas system, which is associated with slip between liquid phase and mixture, depends on the velocity of the mixture and properties of liquid and gas phases. In this study, the following equation (Equation 17) is used to define the drift velocity for the gas-liquid system:

$$v_d^{gl} = \frac{V_d^{gl} + (C_0 - 1)v_m}{\left[1 - (C_0 - 1)\alpha_g \frac{(\rho_l - \rho_g)}{\rho_m} \right]} \quad (17)$$

In which C_0 is the profile parameter and is associated with the distribution of the liquid phase along cross sectional area of flow.

In a similar fashion and for the condensate/water system we have:

$$v_d^{cw} = \frac{V_d^{cw} + (C'_0 - 1)v_l}{\left[1 - (C'_0 - 1)\alpha_c \frac{(\rho_c - \rho_w)}{\rho_l} \right]} \quad (18)$$

The key points to note are that interphase forces terms are canceled out and only wall friction forces are left, and all velocity terms depend on the

mixture velocity v_m . Therefore, the actual unknown parameters are reduced to the following terms: α_g , α_c , α_w , P , and v_m .

Closure Laws

Closure laws assist drift flux model to deliver a better approximation of real flow conditions. In addition, closure laws are needed to close the system as the number of equations should be equal to the number of unknowns. Therefore, it is important to ensure that the applied closure laws in the model are valid for the specified conditions. In addition, closure laws can be determined experimentally or using theoretical equations. These closure models include: density, viscosity, and friction of phases.

Density

Liquid, water, and gas density is assumed to be:

$$\rho_c = \rho_{c0} + \frac{P - P_{c0}}{a_c^2} \quad (19)$$

$$\rho_w = \rho_{w0} + \frac{P - P_{w0}}{a_w^2} \quad (20)$$

$$\rho_g = \frac{P}{a_g^2} \quad (21)$$

where, $a_i \left(\frac{m}{s} \right)$ is the velocity of sound in each phase, and $\rho_{i0} \left(\frac{kg}{m^3} \right)$ and P_{i0} are reference density and pressure values respectively.

The above equations are later coupled with the Peng-Robinson equation of state to model the impact of pressure and temperature changes on phase densities.

Gravitational Forces

Gravitational forces are calculated as a function of well inclination, and the density of the fluids mixture (as seen in Equation 22):

$$F_g = \rho_m g \sin(\theta) \quad (22)$$

Frictional Forces

Contact between the fluids and the wellbore walls cause shear forces. These forces (F_w) are determined using the Fanning equation for each phase (F_{wi}) (as seen in Equation 23):

$$F_{wi} = \frac{f}{2D} \rho_m u_m |u_m| \quad (23)$$

The friction factor f adopted in this work is based on Churchill's correlation [4] (as seen in Equations 24):

$$f = 8 \left(\left(\frac{8}{Re} \right)^{12} + \frac{1}{(A+B)^{15}} \right)^{\frac{1}{12}} \quad (24)$$

and the variables, A and B can be calculated using the following equations (Equations 25 and 26):

$$A = \left(-2.457 \ln \left(\left(\frac{7}{Re} \right)^{0.9} + 0.27 \frac{\varepsilon}{D} \right) \right)^{16} \quad (25)$$

$$B = \left(\frac{37530}{Re} \right)^{16} \quad (26)$$

where ε and D are the pipe's roughness and its internal diameter respectively. The Reynolds number is calculated based on the mixture properties (as seen in Equation 27):

$$Re = \frac{\rho_m v_m D}{\mu_m} \quad (27)$$

The Finite Volume Method and AUSMV Scheme

A recent trend in the development of upwind schemes has been to construct hybrid flux-difference-splitting (FDS) and flux-vector-splitting (FVS) schemes where one tries to combine the accuracy of FDS in the resolution of contact discontinuities and the robustness of FVS in the capturing of stronger discontinuities. For an overview of different implementations of such ideas for calculation of single-phase inviscid flow (Euler Equations) as well as viscous flow (Navier–Stokes), in this study, it is referred to to Evje et al in

2003, and it is referenced therein [6].

The three-phase model explored here is written in the following conservative vector form (as seen in Equation 28):

$$\frac{\partial w}{\partial t} + \frac{\partial F(w)}{\partial x} = S(w) \quad (28)$$

Several basic upwind schemes have been proposed, and most of them are categorized as either FDS or FVS. The former is based on using an exact or approximate solution of the local Riemann problem [7], while the latter typically splits the flux vector into upstream and downstream traveling components according to the sign of its eigenvalues.

FDS is based on matrix calculations, while FVS is based on scalar calculations. Consequently, FVS is more efficient than FDS; however, it introduces excessive numerical dissipation. During the past few years much of research has been done on the Euler Equations motivated by the desire to combine the efficiency of FVS and the accuracy of FDS. The idea is to eliminate surplus dissipation of the FVS by introducing the flavor of the FDS into FVS schemes.

Also, AUSMV in multiphase flow is the extension of flux-splitting schemes previously investigated for Euler and Navier–Stokes calculations to solve for unsteady compressible liquid and gas flow in a pipe. In particular, the performance of an FVS type scheme, a Van Leer type scheme, and an advection upstream splitting method (AUSM) type scheme for the multi-phase model was considered. This scheme is obtained through natural extensions of corresponding single-phase schemes proposed by Wada and Lieu in 1997 [1].

AUSMV is based on FVS scheme. The numerical FVS flux has two components (convective and pressure

fluxes) and at the interface $j+1/2$ is given by the following expression (as seen in Equation 29):

$$F_{j+1/2}^{FVS}(w_L, w_R) = (\alpha_g \rho_g)_L \Theta_{g,L}^+ + (\alpha_g \rho_g)_R \Theta_{g,R}^- + (\alpha_c \rho_c)_L \Theta_{c,L}^+ + (\alpha_c \rho_c)_R \Theta_{c,R}^- + (\alpha_w \rho_w)_L \Theta_{w,L}^+ + (\alpha_w \rho_w)_R \Theta_{w,R}^- + (F_p)_{j+1/2} \quad (29)$$

$F_p = (0, 0, 0, P)^T$ is pressure flux term, L and R represent the left and right part of the control volume respectively and Ψ is velocity function term.

For gas phase:

$$\Psi_{g,L}^+ = \Psi_g^+(v_{g,L}, c_{j+1/2}), \quad \Psi_{g,R}^- = \Psi_g^-(v_{g,R}, c_{j+1/2})$$

$$\Psi_g^+(v, c) = V^+(v, c) \begin{pmatrix} 1 \\ 0 \\ 0 \\ v \end{pmatrix}, \quad \Psi_g^-(v, c) = V^-(v, c) \begin{pmatrix} 1 \\ 0 \\ 0 \\ v \end{pmatrix} \quad (30)$$

For condensate phase:

$$\Psi_{c,L}^+ = \Psi_c^+(v_{c,L}, c_{j+1/2}), \quad \Psi_{c,R}^- = \Psi_c^-(v_{c,R}, c_{j+1/2})$$

$$\Psi_c^+(v, c) = V^+(v, c) \begin{pmatrix} 0 \\ 1 \\ 0 \\ v \end{pmatrix}, \quad \Psi_c^-(v, c) = V^-(v, c) \begin{pmatrix} 0 \\ 1 \\ 0 \\ v \end{pmatrix} \quad (31)$$

For water phase:

$$\Psi_{w,L}^+ = \Psi_w^+(v_{w,L}, c_{j+1/2}), \quad \Psi_{w,R}^- = \Psi_w^-(v_{w,R}, c_{j+1/2})$$

$$\Psi_w^+(v, c) = V^+(v, c) \begin{pmatrix} 0 \\ 0 \\ 1 \\ v \end{pmatrix}, \quad \Psi_w^-(v, c) = V^-(v, c) \begin{pmatrix} 0 \\ 0 \\ 1 \\ v \end{pmatrix} \quad (32)$$

In the Equations 30-32, the V^\pm is defined as:

$$V^\pm = \begin{cases} \pm \frac{1}{4c} (v \pm c)^2 & \text{if } |v| \leq c, \\ \frac{1}{2} (v \pm |v|) & \text{if } |v| > c \end{cases} \quad (33)$$

The FVS type discretization for the pressure term F_p is given as:

$$P_{j+1/2} = P^+(v_L, c_{j+1/2})P_L + P^-(v_R, c_{j+1/2})P_R \quad (34)$$

where $c_{j+1/2}$ is the sound velocity at volume interface and v is mixture velocity; moreover, splitting

pressure is defined as:

$$P^\pm(v, c) = V^\pm(v, c) \cdot \begin{cases} \frac{1}{c} \left(\pm 2 - \frac{v}{c} \right) & \text{if } |v| \leq c, \\ \frac{1}{v} & \text{if } |v| > c \end{cases} \quad (35)$$

The sound velocity c related to the gas-liquid mixture is expressed by the following equations which are used to find approximated sound velocity:

$$c(\alpha_g) = \begin{cases} \min(a_l, \omega) & \text{if } a_g < 0.5 \\ \min(a_g, \omega) & \text{if } a_g \geq 0.5 \end{cases} \quad (36)$$

In which ω is approximate sound velocity in multiphase system as a function of pressure (P) and gas volume fraction (a_g) (as seen in Equation 37):

$$\omega^2 = \frac{P}{a_g \rho_l (1 - K a_g)} \quad (37)$$

Although the speed of sound can be estimated more accurately by robust approximation, in order to simplify the model, the above method has been considered for this study.

In AUSMV scheme, the velocity splitting formula V^\pm is replaced by \tilde{V}^\pm with a weighing factor χ which is given by the following expression:

$$\tilde{V}^\pm(v, c, \chi) = \begin{cases} \chi V^\pm + (1 - \chi) \frac{v \pm |v|}{2} & \text{if } |v| \leq c, \\ \frac{1}{2} (v \pm |v|) & \text{if } |v| > c \end{cases} \quad (38)$$

The parameter χ can be specified in many different ways and in this study the following choice as per Evje et al 2003 is used [6]:

$$\chi_L = \alpha_R, \quad \chi_R = \alpha_L \quad (39)$$

AUSMV Scheme Extension to Three-phase

By considering the simple model for the density of liquids and gas and combining the conservative law elements in Equation 5 to Equation 8, an analytic model for pressure is derived. The derivation steps are as follows:

It is shown that:

$$\rho_c \rho_w w_g + \rho_g \rho_w w_c + \rho_g \rho_c w_w = \rho_g \rho_c \rho_w (\alpha_g + \alpha_c + \alpha_w) = \rho_g \rho_c \rho_w \quad (40)$$

By replacing the density terms in Equation 40 with its simple models represented in Equations 19 to 21, and solving for P, polynomial of Equation 41 is formulated.

$$k_1 a_1 b_1 P^3 + (k_1 a_1 b_2 + k_1 a_2 b_1 - (a_1 b_1 w_g + k_1 b_1 w_c + k_1 a_1 w_w)) P^2 + (k_1 a_2 b_2 - (a_1 b_2 w_g + k_1 b_2 w_c + k_1 a_2 w_w)) P - a_2 b_2 w_g = 0 \quad (41)$$

In which:

$$k_1 = \frac{1}{a_g^2}, a_1 = \frac{1}{a_c^2}, a_2 = \frac{-P_0 + \rho_c a_c^2}{a_c^2}, b_1 = \frac{1}{a_w^2}, b_2 = \frac{-P_0 + \rho_w a_w^2}{a_w^2} \quad (42)$$

The maximum root of equation 41 is the model prediction of pressure for each volume. The results are in very good agreement with those presented by Udegbumam et al in 2015 for the simulation of two phase flow [2].

Boundary and Initial Conditions

Since governing equations are first derivatives in time and space, one initial and one boundary condition is necessary to close the system of equations. These two conditions are defined as per assumed condition of a blowout. In addition, the AUSMV hybrid scheme uses a simpler extrapolation method for pressure fluxes. At the inlet boundary, the mass flow rates of liquid and gas are known; hence, the convective fluxes are given directly. The inlet pressure flux, P_{inlet} , is found by extrapolation, with the pressures in the first two adjacent cells. This explains the effects which are related to dominant source terms such as gravity and friction:

$$P_{inlet} - P(1) + 0.5[P(1) - P(2)] \quad (43)$$

Open-end conditions can be specified at the outlet boundary. For the open conditions, the convective fluxes are calculated with the outlet-cell primitive

variables (phase densities, volume fractions, and velocities). The outlet-pressure flux is set to the atmospheric pressure of 100 kPa.

Flow-area Discontinuities

AUSMV uses an approach for treating the flow area changes to obtain the correct results because of difficulty associated with the discretization of the source terms. The main idea is to place the flow-area discontinuity at the center of a cell, and then apply mass-balance requirements. The following equations represent the fluid-mass conservations (as seen in Equations 44 to 46):

$$(A \alpha_g \rho_g v_g)_L = (A \alpha_g \rho_g v_g)_R \quad (44)$$

$$(A \alpha_c \rho_c v_c)_L = (A \alpha_c \rho_c v_c)_R \quad (45)$$

$$(A \alpha_w \rho_w v_w)_L = (A \alpha_w \rho_w v_w)_R \quad (46)$$

Pressure and corresponding density of each phase are assumed constant across the discontinuity, whereas the volume fraction is averaged.

Thermodynamic Model

Thermodynamic modeling consists of two major parts, (1) first, density and viscosity of fluids are calculated using the Peng-Robinson equation of state. It should be noted that the Peng-Robinson equation has been used here as an example of a thermodynamic model and other methods can be used in a similar form of fashion. (2) Then, energy equation over cell volume is solved using an iterative approach to achieve a better approximation of fluid temperature profile in each time step.

Density and Viscosity Update

The density of gas, condensate, and water is calculated using the Peng-Robinson Equation of state. Binary interaction numbers are derived

from PVT and phase behavior of reservoir fluids, but volume shift for liquid density is ignored. In cases that condensate is in two phase, the liquid phase density is accepted by an assumption that the calculated volume fraction of gas in the hydrodynamic model will cover the vapor part. Since the simple model of density is already used to predict the system pressure, the calculated density cannot be directly incorporated into the flow model, so it is used as a correction to the used sound velocity in the simple density model as shown in Equations 47 to 49.

$$\alpha_c^2 = \frac{P - P_{c0}}{(\rho_{c, \text{calculated on PR}} - \rho_{c0})} \quad (47)$$

$$\alpha_w^2 = \frac{P - P_{c0}}{(\rho_{w, \text{calculated on PR}} - \rho_{w0})} \quad (48)$$

$$\alpha_g^2 = \frac{P}{\rho_{g, \text{calculated}}} \quad (49)$$

Based on the geometric similarity of P-V-T, T-μ-P diagrams, viscosity μ data of hydrocarbons and their mixtures have been successfully correlated using a cubic equation of state (EOS). A modified viscosity correlation based on Peng-Robinson. An EOS type expression is used to predict viscosity of fluid [8] within the calculated pressure and temperature. Moreover, EOS type expression is directly implemented into the flow model to update friction and other viscosity related parameters.

Energy Equation, Enthalpy Calculation, and Temperature Prediction

In this study, the potential difference between the temperature of the flowing fluid and fluid at rest has been ignored. The energy equation to obtain the fluid temperature in a wellbore is the total energy conservation:

$$\begin{aligned} & \frac{\partial \left[\alpha_g \rho_g \left(h_g + \frac{v_g^2}{2} \right) \right]}{\partial t} + \frac{\partial \left[\alpha_c \rho_c \left(h_c + \frac{v_c^2}{2} \right) \right]}{\partial t} + \frac{\partial \left[\alpha_w \rho_w \left(h_w + \frac{v_w^2}{2} \right) \right]}{\partial t} + \\ & \frac{\partial \left[\alpha_g \rho_g v_g \left(h_g + \frac{v_g^2}{2} \right) \right]}{\partial x} + \frac{\partial \left[\alpha_c \rho_c v_c \left(h_c + \frac{v_c^2}{2} \right) \right]}{\partial x} + \frac{\partial \left[\alpha_w \rho_w v_w \left(h_w + \frac{v_w^2}{2} \right) \right]}{\partial x} + \\ & \left(\alpha_g \rho_g v_g + \alpha_c \rho_c v_c + \alpha_w \rho_w v_w \right) g \sin \theta \\ & - H_g - H_c - H_w + \frac{\dot{Q}}{A} = 0 \end{aligned} \quad (50)$$

The energy equation is discretized using first order finite difference method and solved with one cycle time lag with regard to pressure. So in each simulation cycle, all parameters are known except the enthalpies which are functions of known pressure and unknown temperature. Therefore, Equation 50 will be reduced (or simplified) to find the roots of Equation 51.

$$C_1 h_g + C_2 h_c + C_3 h_w + C_4 = 0 \quad (51)$$

In Equation 50, \dot{Q} is the heat exchange per unit length, between the fluid and the surrounding formation. This term is defined as follows (as seen in Equation 52):

$$\dot{Q} = 2\pi r_o U_t (T - T_{wb}) \quad (52)$$

where U_t is the overall heat transfer coefficient, T is the fluid temperature, r_o is the casing outer radius, and T_{wb} is the formation temperature at the vicinity of the wellbore.

The enthalpy, h, for each phase is calculated as the sum of two contributors' enthalpy: the ideal gas enthalpy and residual enthalpy, h^{res} (as seen in Equation 53):

$$h = \sum_1^n x_i h_i^{id} + h^{res} \quad (53)$$

where n is the number of components, x_i is the mole fraction of component i in the phase considered, and h_i^{id} is the molar ideal gas enthalpy of component i (as seen in Equation 54).

$$h_i^{id} = \int_T^{T_{ref}} C_{pi}^{id} dT \quad (54)$$

T_{ref} is a reference temperature (273.15 K). C_{pi}^{id} is the molar ideal gas enthalpy of component i , which is calculated from a third degree polynomial in temperature, as seen in Equation 55:

$$C_{pi}^{id} = C_{(1,i)} + C_{(2,i)}T + C_{(3,i)}T^2 + C_{(4,i)}T^4 \quad (55)$$

The values used for the coefficients C1-C4 of the lighter petroleum mixture constituents are those recommended by Reid et al in 1997 [9]. For C_{7+} hydrocarbon fractions C1-C4 are for heat capacities calculated from the correlations [10].

The residual term of h is derived from the Peng Robinson Equation of state using the following general thermodynamic relation (as seen in Equation 56):

$$h^{res} = -RT^2 \frac{\partial \ln \phi}{\partial T} \quad (56)$$

Parameters C1-C4 in Equation 51 are calculated using an iterative method by guessing initial temperature, calculating enthalpies and calculating Equation 51 and finding the variances. This method provides us with a robust temperature calculation. Moreover, the calculated temperature is used for the next step of simulation to update density and viscosity parameters.

RESULTS AND DISCUSSION

Model Comparison

Due to lack of data for the three phase system, the model presented here has been validated in two steps. Due to the importance of the input parameters, at first the thermodynamic gas properties predicted by this model has been compared to that of a commercial software. As expected, the model predicts identical results as those produced with PVTsim (Figure 1)

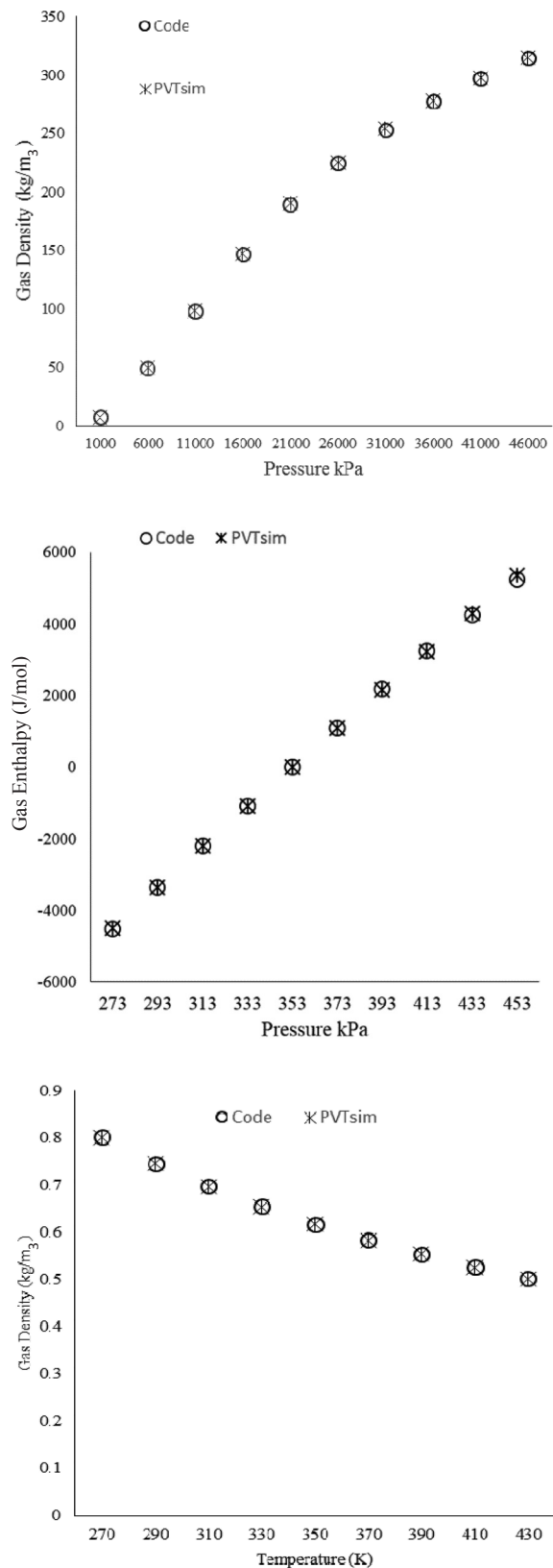


Figure 1: Validation of gas density as a function of pressure, gas enthalpy, and its density as a function of temperature.

In addition, the results of this new model has been compared to a two phase model published by Udegbunam et al in 2015 [2]. In their study, the ASUMV in combination with (1) FVS and (2) drift flux to model a two-phase system has been used by Udegbunam et al in 2015. Both of the studies, i.e. the current study and the study conducted by Udegbunam et al in 2015, are showing the numerical capability of the ASUMV hybrid algorithm. Applying similar boundary and initial conditions and taking into account the assumptions made by Udegbunam et al in 2015, a two phase system has been simulated and compared to their results. As expected both models should predict similar results (Figures 2) [2].

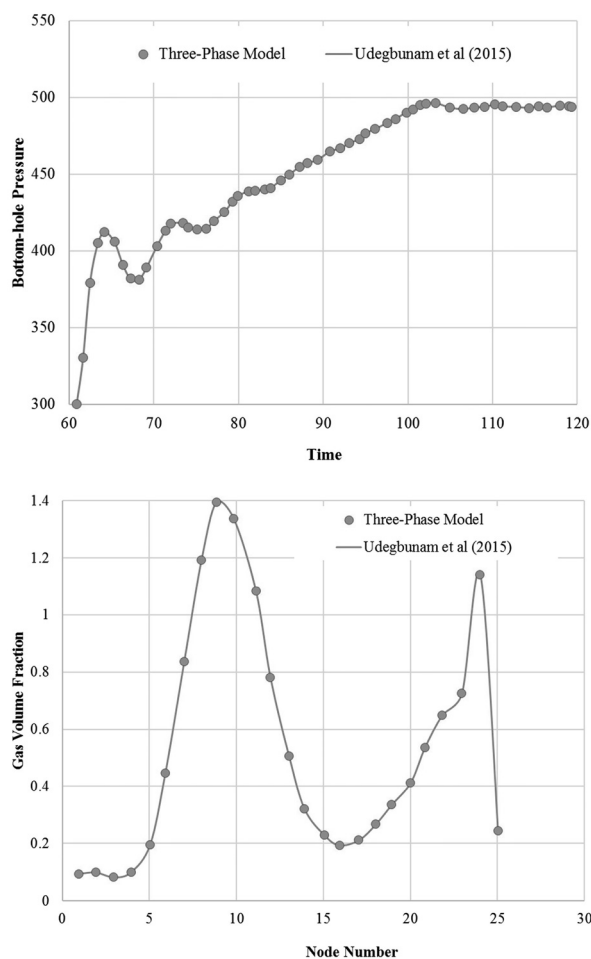


Figure 2: Bottom-hole pressure and volume fraction comparison between the new model and model presented by Udegbunam et al in 2015.

Dynamic Kill Simulation Case

The simulation process consists of four main steps: initialization, steady state conditions, blowing simulation, and dynamic kill operation.

First, initial and boundary conditions as shown in Tables 1 and 2 are applied. In the second step, by increasing gravity value from zero to 9.81 within 100 s the steady state of well containing just water is simulated. In the third step, the productivity index (PI) model starts and gradually the J factor is increased to simulate the blowout. After reaching stable blowout condition in around t=300 seconds, the relief well mass enters the well and dynamic kill operation starts until the bottom hole pressure exceeds the reservoir pressure, and PI model influx stops.

In each loop of simulation after calculation of interim fluxes, conservative variables are calculated. Then new pressure is derived based on Equation 6. Afterward, density, volume fraction, and mixture viscosity values are updated for the next loop of simulation. To calculate the velocity of each phase, a drift velocity model for gas and liquid is implemented. Mixture velocity is calculated from conservative parameters and calculated pressure, then the phase velocity is determined.

Table 1: Boundary conditions.

Boundary description	Boundary Value
Well Outlet Pressure	100,000 Pa
Well Outlet Temperature	293 K
Bottom hole Pressure	Linear extrapolation of 2 nodes above the bottom
Bottom hole Temperature	373 K

Initial fluid properties' values are set as per Table 2.

Table 2: Initial values.

Phase	Density (ρ) (Kg/m ³)	Viscosity (μ) (Poise)	Sound Speed (a) (m/s)
Gas	0.7367	1.13e-5	420
Condensate	729	5e-4	1005
Water	998	1e-3	1500

The well consists of a casing diameter of 0.2167 m and drill string outer diameter of 0.127 m with a measured depth of 4000 m. Moreover, to represent the drill collar outer diameter of 0.168 m is selected in the two first sections of the Bottom-hole. The relief well is considered as a point of injection of water into node number 1 (bottom hole) and the mass rate of injection (as an example: 280 kg/s) is set at the time of injection (t=300 second onward) as a boundary value within water flux equation. In addition, to avoid fluctuation in calculated pressure with regard to the sudden increase of mass flux of water, it is gradually raised from zero to 280 kg/s within 100 seconds and remains unchanged afterward. By monitoring the values of bottom hole pressure and gradually increasing mass rate, the optimum range can be found. The schematics of the well is shown in Figure 3.

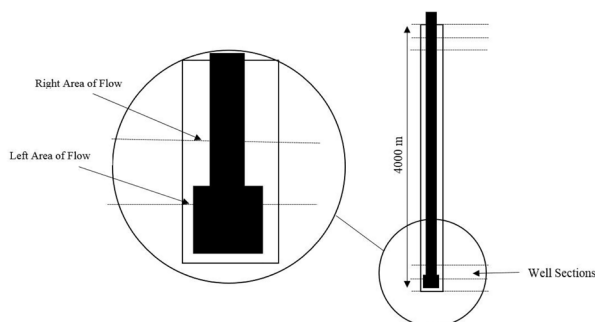


Figure 3: Well geometry used for the simulation study.

The initial temperature gradient is a linear gradient starting from 373 K at Bottom-hole to 293 K at the surface. It is assumed that the temperature profile of the well is the same as the mentioned initial gradient but may change according to the flow

properties and the result of fluid energy changes. The drift velocity, v_{gl}^d is set to 0.5 and drift coefficient, C_o is set to 1.2, and velocity of water and condensate phase are set equal, but the model and simulator built based on this model can handle the separation of velocities if the proper experimental coefficient is found.

In order to evaluate the model, the values of $J_g = 1 \times 10^{-7} \left(\frac{m^3/s}{Pa} \right)$ and $J_c = 1 \times 10^{-6} \left(\frac{m^3/s}{Pa} \right)$ are considered as examples. Reservoir pressure is set to 500 bar, and it is assumed that well perforation is in node number 3.

Also, to avoid a high influx of liquid and gas at a short time, the values of J is gradually increased within 50 seconds from zero to target values. Moreover, this method will allow a smoother result.

Figure 4 represents the algorithm of simulation within blowing well during dynamic kill operation.

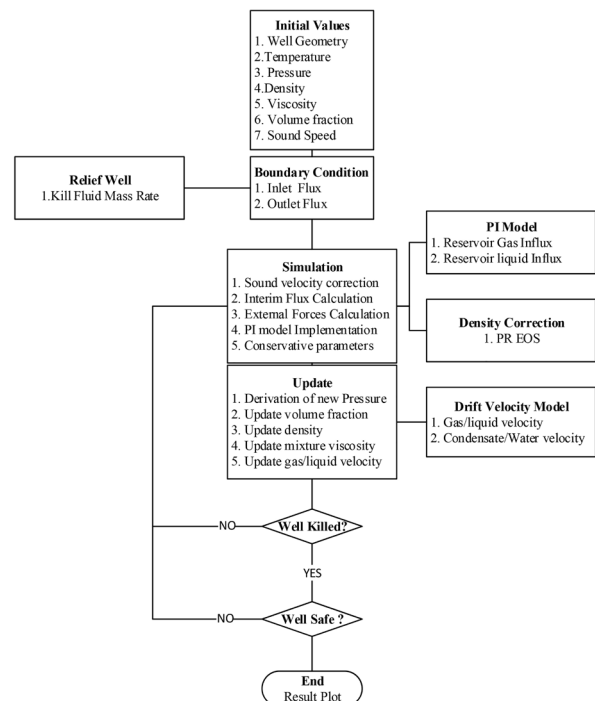


Figure 4: Modeling Flowchart.

Bottom hole pressure is monitored, and the result is shown in Figure 5.

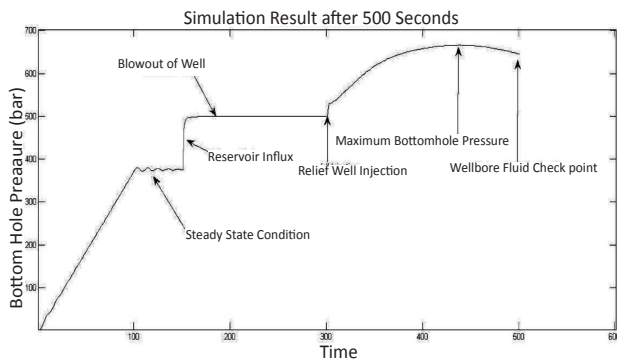


Figure 5: Bottom Hole Pressure.

The steady state condition of the well shows a 374 bar pressure at the bottom hole. As the reservoir pressure is 500 bar, based on the PI model, gas and condensate flow into the wellbore. This influx increases the pressure to 499.5 bar, which is the blowout pressure. At $t=300$ seconds, relief well starts the mass rate of 280 kg/s of water into the wellbore. This causes a rapid increase in the pressure above the reservoir pressure and reservoir influx stops. Although there is no more influx from the reservoir, wellbore is still full of reservoir fluid, so simulation continues and at $t=500$ almost half of the wellbore is filled with water. The volume fraction of water is shown in Figure 6.

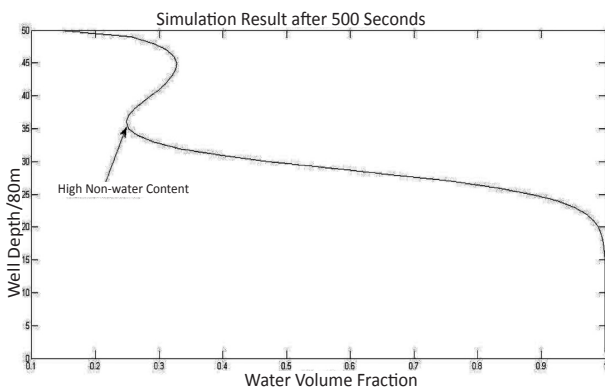


Figure 6: Volume fraction of water across well depth at 500 seconds.

Thus, the pressure tends to back to its value before the blowout, and the curvature of pressure graph in Figure 5 approves this. Fluid velocity profile at 500 seconds is plotted in Figure 7.

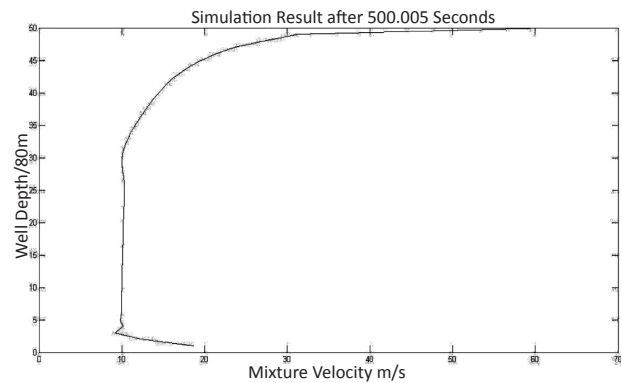


Figure 7: Mixture velocity across well depth at 500 seconds.

As the near surface fluid gas content is high, and pressure is also much more than atmospheric pressure, sudden release to the atmosphere will cause high speed at the surface which is proven by results at the upper section of the velocity profile.

Sensitivity Analysis on Kill Fluid Rate

Sensitivity analysis of kill rate and its effect on kill time, and bottom hole pressure is demonstrated as shown in Figure 8.

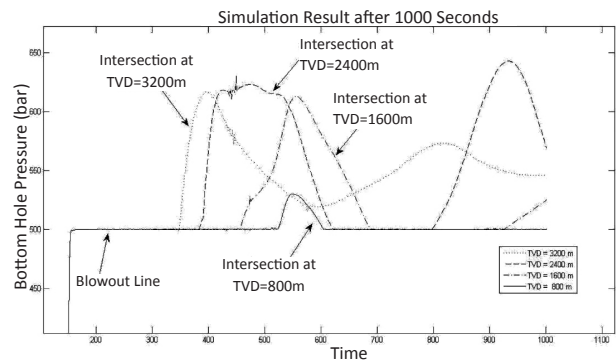


Figure 8: Sensitivity analysis of kill rate on kill time and maximum pressure.

The kill rate below 150 kg/s will not kill the blowing well. By increasing kill rate, killing time is decreased, but the availability of pumps to overcome the required pressure must be considered. Bottom-hole pressure during kill is increased and then decreased and to a minimum and going up and become steady at a fixed pressure, so the best point

of ending the operation could be the minimum section to avoid any damage to the formation. Achieving this point depends on the kill rate. The kill rate of 250 kg/s happens in around 600 seconds of simulation. In the mentioned simulation scenario, temperature update of fluids is not considered.

Sensitivity Analysis on Intersection Depth

A sensitivity analysis of intersection depth of relief well with blowing well is performed at the rate of 200 kg/s, and Bottom-hole pressure is monitored for 1000 seconds. The result is shown in Figure 9.

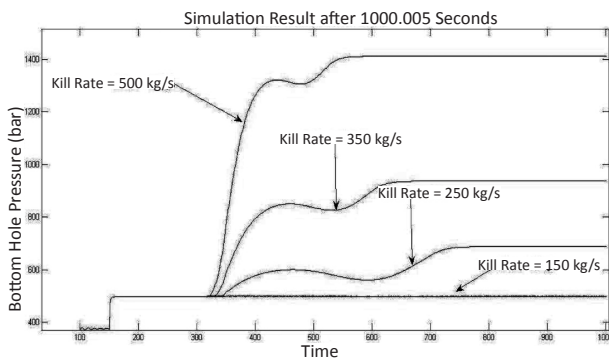


Figure 9: Sensitivity analysis of relief well intersection on Bottom-hole pressure.

Intersection point of relief well and blowing well have a direct effect on the kill time with the same kill fluid. As shown in Figure 9, a kill rate of 200 kg/s with the intersection of 3200 m kills the well at 350 s, and the Bottom-hole pressure remains always upper than blowing pressure which means the well is dead and is not blowing more.

The intersection of 1600 m causes a later kill time and the Bottom-hole pressure remains high for a longer time, maybe because of remaining reservoir fluid compression in wellbore, after a while Bottom-hole pressure drops sharply and a blowout starts again and the kill cycle starts again. For intersection of 800 which is so close to surface, the chance of kill is as low as a short period of time Bottom-hole

pressure increases reservoir pressure, but the well could not be filled with water, well is blowing again after a while. The deeper the intersection, the less kill time is suggested by this sensitivity analysis but the deeper the intersection, the less kill time could not be suggested and considered as a rule because transient flow simulations depend on so many parameters.

Thermodynamic Effects

The effect of density and viscosity correction on Bottom-hole pressure prediction is shown in Figure 10.

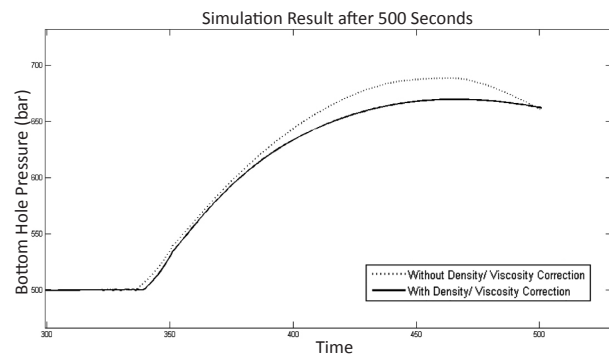


Figure 10: Effect of density/viscosity correction on Bottom-hole pressure.

In simulation case without density and viscosity correction, the predicted Bottom-hole pressure during a blowout is almost the same as a simulation with applied density, viscosity change, but in the dynamic kill operation, the significant variance is detected which shows the importance of density and viscosity correction with respect to updated pressure and temperature.

CONCLUSIONS

A transient three phase model to capable of capturing flow parameters during dynamic kill of gas-condensate well is developed based on AUSMV scheme and coupled with a thermodynamic model to include the effect of temperature on

density, viscosity, and temperature of flowing fluid. Moreover, a blowout scenario is defined, and dynamic kill operation is successfully simulated. The state of safe and killed well is discussed through trend and sensitivity analysis of the parameters. In addition, this model can also be used for training and educational purposes. Finally, field data can be used in the future works to prove the practical relevance of the theoretical model and compare the model predictions with simulation and experimental results from previous studies.

ACKNOWLEDGMENTS

Authors would like to thank the Stavanger University for its knowledge sharing of their academic researches.

NOMENCLATURES

AUSMV	: Advection-Upstream-Splitting-Method
α	: volume fraction dimensions
ρ	: density, kg/m ³
Γ	: mass exchange rate, kg/s.m ³
FDS	: flux-difference splitting
FVS	: flux-vector splitting
CFL	: Courant-Friedrichs-Lewy
EOS	: Equation of State
H	: enthalpy influxes per unit well
g	: acceleration caused by gravity, m/s ²
R	: gas constant, J/mol.K
PI	: Productivity Index

APPENDIXES

Appendix 1

This section covers the numerical discretization and approaches applied to the ASUMV in this study. An explicit method to solve Equation 5 is

used. First, the AUSMV fluxes at the cell interfaces are established before the calculation of the conservative variables at a new time level are using the values at the old time level.

The following expression (Expression 1) is used to determine the variables at the new time level:

$$w_j^{n+1} = w_j^n - \frac{\Delta t}{\Delta x} \left(F_{j+\frac{1}{2}}^{AUSMV} - F_{j-\frac{1}{2}}^{AUSMV} \right) - \Delta t q^n \quad (1)$$

Time step (Δt) is limited by the CFL condition because the fluxes are treated explicitly in time [11]. The CFL condition is a stability requirement for the scheme, and The CFL condition should always be lower than 1.

The CFL condition for the scheme is given by the following expression (Expression 2):

$$\Delta t = CFL \frac{\Delta x}{\max(|\lambda_1|, |\lambda_2|, |\lambda_3|)} \quad (2)$$

In which, the following expressions are obtained (Expression 3):

$$\lambda_1 = v_l - \omega, \quad \lambda_2 = v_g, \quad \lambda_3 = v_l + \omega \quad (3)$$

REFERENCES

1. Wada Y. and Liou M. S., "An Accurate and Robust Flux Splitting Scheme for Shock and Contact Discontinuity," *SIAM Journal Science Computer*, **1997**, 18(3), 633–657.
2. Udegbumam J. E., Fjelde K. K., Evje S., and Nygaard G., "On the Advection-Upstream Splitting- Method Hybrid Scheme: A Simple Transient-Flow Model for Managed-Pressure-Drilling and Underbalanced-Drilling Applications," *SPE Drilling and Completion*, **2015**, 30(02), 98-105.
3. Soprano A. B., Ribeiro G. G., da Silva A. F. C., and Maliska C. R., "Solution of a One-dimensional Three-phase Flow in Horizontal Wells Using a Drift-flux Model," *Mecánica Computacional*

- Journal*, **2010**, *29*, 8767-8779.
4. Hibiki T. and Ishii M., "One-dimensional Drift-flux Model and Constitutive Equations for Relative Motion between Phases in Various Two-phase Flow Regimes," *International Journal of Heat and Mass Transfer*, **2003**, *46*(10), 1773-1790.
 5. Churchill S. W., "Comprehensive Correlating Equations for Heat, Mass and Momentum Transfer in Fully Developed Flow in Smooth Tubes," *Industrial Engineering Chemistry Fundamental*, **1977**, *16*(1), 109–116.
 6. Evje S. and Fjelde K. K., "On a Rough AUSM Scheme for a One-Dimensional Two-Phase Model," *Computers and Fluids Journal*, *32*(10), **2003**, 1497-1530.
 7. Osher S. "Riemann Solvers, the Entropy Condition, and Difference," *SIAM Journal on Numerical Analysis*, **1984**, *21*(2), 217-235.
 8. Guo X. Q., Sun C. Y., Rong S. X., Chen G. J., and et al., "Equation of State Analog Correlations for the Viscosity and Thermal Conductivity of Hydrocarbons and Reservoir Fluids," *Journal of Petroleum Science and Engineering*, **2001**, *30*, 15–27.
 9. Reid R. C., Prausnitz J. M., and B. E. Poling, "The Properties of Gases and Liquids (4th ed.), McGraw-Hill, New York, **1987**.
 10. Kesler M. G. and Lee. B. I., "Improved Prediction of Enthalpy of Fractions," *Hydrocarbon Processing*, **1976**, 153-158.
 11. Courant R., Friedrichs K., and Lewy H., "Über Die Partiellen Differenzgleichungen der Mathematischen Physik," *Mathematische Annalen* (in German), **1928**, *100*(1), 32-74.